PHYSICAL REVIEW E **72**, 030101(R) (2005)

Lambert diffusion in porous media in the Knudsen regime: Equivalence of self-diffusion and transport diffusion

Stefanie Russ,[1] Stephan Zschiegner,[1,2] Armin Bunde,[1] and Jörg Kärger[2]
[1]*Institut für Theoretische Physik III, Justus-Liebig-Universität Giessen, D-35392 Giessen, Germany*
[2]*Fakultät für Physik und Geowissenschaften, Universität Leipzig, D-04103 Leipzig, Germany*
(Received 19 November 2004; revised manuscript received 15 July 2005; published 9 September 2005)

We study molecular diffusion in nanopores with different types of roughness under the exclusion of mutual molecular collisions, i.e., in the so-called Knudsen regime. We show that the diffusion problem can be mapped onto Levy walks and discuss the roughness dependence of the diffusion coefficients D_s and D_t of self- and transport diffusion, respectively. While diffusion is normal in $d=3$, diffusion is anomalous in $d=2$ with $D_s \sim \ln t$ and $D_t \sim \ln L$, where t and L are time and system size, respectively. Both diffusion coefficients decrease significantly when the roughness is enhanced, in remarkable disagreement with earlier findings.

DOI: 10.1103/PhysRevE.72.030101 PACS number(s): 05.40.Fb, 47.55.Mh, 66.30.Pa

Diffusion and transport phenomena of gases in disordered and porous media have been subject to intense research for several decades [1–4]. Among the experimental and technical applications are heterogeneous catalysis [5], adsorption [6], and separation [7]. Recent progress in synthesizing nanostructured porous materials [6] has provided essentially unlimited options for the generation of purpose-tailored pore architectures. In particular, the recent achievements in fabricating silicon wafers with tubular pores of deliberately structured diameter profiles [8] open up options for producing porous materials with exactly recorded structural details in the near future. In addition, in matter conversion and separation, as two prominent technical applications, bimodal porous materials have attained particular attention. These materials contain "transport pores" that ensure fast molecular exchange between the microporous regions, in which the actual conversion and separation phenomena take place [9].

In general, the diffusion of the gas molecules through the pores depends on the collisons between the gas molecules as well as on the collisions of the gas with the pore walls. In the transport pores, the so-called Knudsen diffusion dominates, where the interaction of the molecules with the pore walls play the crucial role and the intermolecular collisions can be neglected. In this case, the molecules perform a series of free flights and change the flight direction statistically after collisions with the pore walls. In this paper, we concentrate on this case.

Experimentally, two kinds of diffusion problems can be considered, the so-called transport diffusion, where the particles diffuse in a nonequilibrium situation from one side of the system to the opposite side (here under the influence of a concentration gradient) and the self- (or tracer) diffusion under equilibrium conditions. These problems are described by the transport diffusion coefficient D_t and the self- (or tracer) diffusion coefficient D_s, respectively.

In most cases it is not possible to determine D_t and D_s simultaneously. It is generally assumed that D_s and D_t are equivalent in the Knudsen regime. Deviations between both are normally attributed to intermolecular interactions. For the exploration of the underlying porous material, different techniques of diffusion measurement, including quasielastic neutron scattering [10], pulsed field gradient NMR [11], and interference microscopy [12] have become indispensable tools. Their evidence is often based on structure-related correlations of the experimental data with the different types of molecular diffusion, including self- and transport diffusion. The equivalence between both types of diffusion in the case of Knudsen diffusion is a fundamental prerequisite.

Recently, this equivalence has been questioned by Malek and Coppens [4,13,14], who found by numerical simulations that the self-diffusion coefficients decreased significantly with increasing surface roughness of the pore, whereas the transport diffusion coefficients were insensitive to the shape of the boundary. If these findings were correct, most experimental works that are based on the above techniques would have to be reinterpreted.

In this paper, we use scaling arguments and numerical simulations to understand how in the Knudsen regime both types of diffusion depend on the morphological details of the pores, in particular on their surface roughness. We show that Knudsen diffusion depends crucially on the dimension d of the system. In the experimentally relevant $3d$ pores, we find that diffusion is normal, while for $2d$ pores, D_s depends logarithmically on time t, and D_t depends logarithmically on the lenghth L of the pore. Contrary to the findings of [4,13,14], both D_s and D_t decrease monotonically with increasing surface roughness.

In the numerical simulations, the particles start at the left side of the pore when transport diffusion is considered or in the middle of the pore when self-diffusion is considered. Each particle performs a random trajectory inside the pore, where it moves with constant velocity u_0 along the trajectory. When the particle hits the pore boundaries, it is absorbed for a very short while and then emitted into a new random direction. This new direction is chosen according to Lambert's cosine law, where the new angle $\vartheta \in [-\pi/2, \pi/2]$ to the normal component of the surface occurs with probability $dP(\vartheta, \varphi) \sim \cos \vartheta d\Omega$, where $d\Omega = d\vartheta$ in $d=2$ and $d\Omega = \sin \vartheta d\vartheta d\varphi$ in $d=3$ [15]. The $2d$ and $3d$ pores of different roughness that we consider are built by sticking together n units of equal length and width h, with n up to 2000, which leads to a total length $L=nh$ of the pores. For the smooth

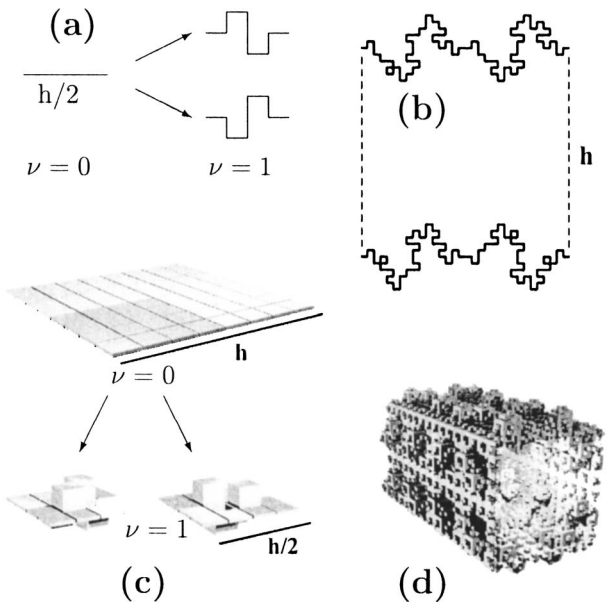

FIG. 1. Geometry of the pores considered in this paper: (a), (c) two realizations of the generalized random Koch curve generator in $d=2$ and 3, respectively. (b) $2d$ pore of length $L=h$ and roughness $\nu=2$. (d) $3d$ pore of length $L=2h$ and roughness $\nu=2$.

pores (generation $\nu=0$), this unit is a square in $d=2$ and a cube in $d=3$. For higher generations ν, the boundary of each unit is created iteratively by a random generalized Koch curve: In each generation all lines (squares) of length $h/2$ are replaced by one of the two realizations of the Koch curve generator [see Figs. 1(a) and 1(c)]. The highest iteration, $\nu=3$, yields the highest roughness considered in this paper. Figures 1(b) and 1(d) show examples of random $2d$ and $3d$ pores, respectively. By construction, the volume of the pores does not depend on ν. In the numerical calculations, we have set the pore width h and the velocity u_0 equal to 1.

The first quantity we are interested in is the distribution $P(|x|)$ of the jump lengths $|x|$ parallel to the channel. Figure 2 shows that asymptotically $P(|x|)$ decays as

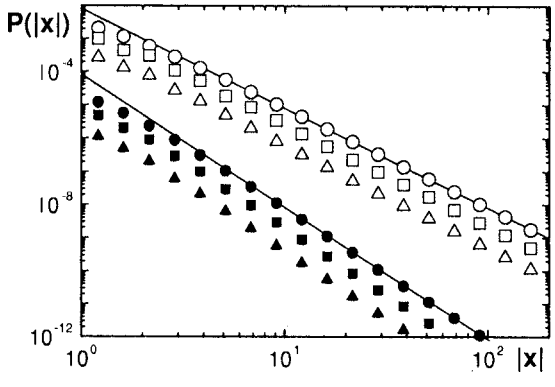

FIG. 2. The distribution $P(|x|)$ is plotted vs $|x|$ for the $2d$ pores (open symbols) and for the $3d$ pores (filled symbols) of $\nu=0$ (circles), $\nu=1$ (squares), and $\nu=3$ (triangles). The data of $d=3$ have been shifted down by a factor of 100. The lines of slopes −3 and −4 are guides to the eye. The average was taken over 10^5 trajectories.

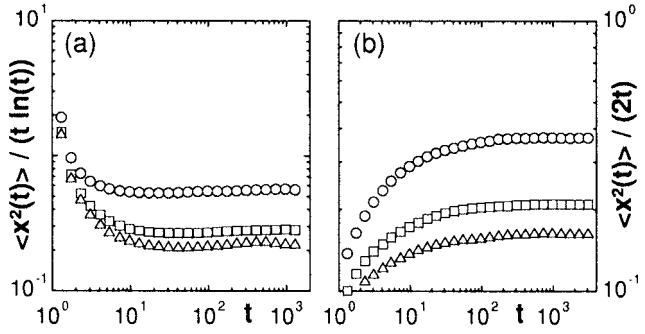

FIG. 3. (a) The scaled mean square displacement $\langle x^2(t)\rangle/(t\ln t)$ (averaged over 10^5 trajectories) is plotted vs t in $d=2$. (b) The self-diffusion coefficient $D_s=\langle x^2(t)\rangle/(2t)$ is plotted vs t in $d=3$. The different symbols indicate different roughness of $\nu=0$ (circles), 1 (squares), and 3 (triangles).

$$P(|x|) \sim |x|^{-(1+\beta)}, \tag{1}$$

with $\beta=2$ for $d=2$ and $\beta=3$ for $d=3$, irrespective of the roughness. For the smooth pore in $d=2$, Eq. (1) can be easily derived analytically.

The behavior of $P(|x|)$ for large jumps determines the diffusion properties at large times. In the $2d$ pores, large jumps occur close to the angles $\vartheta=\pm\pi/2$. In $d=3$ the jump length is determined by ϑ and φ, and only the proper combination of both leads to very large jumps. Naturally, this combined probability is quite small and large jumps are thus very rare.

By definition, the time of each jump is proportional to the jump length l. For very large jumps, we have $x \simeq l$, i.e., the jump time is proportional to the jump length in the x direction, $x \sim t$. Hence, Eq. (1) defines a Levy walk in $d=1$ [16–19]. It is well known [17–19] that for a Levy walk in $d=1$, the mean square displacement scales as

$$\langle x^2\rangle = 2D_s(t)t, \tag{2}$$

where asymptotically

$$D_s(t) = \begin{cases} D_s^0 \ln t & \text{for } \beta = 2, \\ D_s & \text{for } \beta > 2, \end{cases} \tag{3}$$

with proportionality constants D_s and D_s^0. Accordingly, we expect that in $d=2$, where $\beta=2$, the diffusion is anomalous with a diffusion coefficient that depends explicitely on time t and tends to infinity with increasing t. For a direct analytical calculation of $D_s(t)$ see [20]. Hence, when comparing $2d$ systems, it is essential to keep t fixed. In $d=3$, $\beta=3$ and we expect normal diffusion.

To test these predictions, we have simulated the Knudsen diffusion for the different pore geometries. To reveal the logarithmic time behavior of $D_s(t)$ for the $2d$ pores, we plot $\langle x^2(t)\rangle t^{-1}(\ln t)^{-1}$ vs t in Fig. 3(a). For large t, the data reach a plateau, from which we obtain D_s^0 in accordance with Eqs. (2) and (3). The figure also shows that with increasing boundary roughness, the diffusion is considerably slowed. To reveal the normal diffusion behavior in $d=3$, we plot $\langle x^2(t)\rangle/(2t)=D_s$ vs t in Fig. 3(b). Again, the data reach a plateau showing that Eqs. (2) and (3) describe the behavior

correctly. Also in $d=3$, D_s decreases strongly with increasing boundary roughness. It is interesting to note that the relative decrease of D_s^0 in $d=2$ and D_s in $d=3$ are roughly the same.

Next, we consider the related transport diffusion problem, where we assume that a constant concentration gradient $\vec{\nabla}c = -\vec{e}_x c_0/L$ is applied between the concentrations $c=c_0$ at the left-hand side and $c=0$ at the right-hand side of the pore. Particles start at the left wall, perform a random trajectory between the system walls and are absorbed when they hit either the left or the right wall. This leads, after some relaxation time, to a constant current $\vec{J}$. According to Fick's law, the current density $\vec{j}=\vec{J}/h^{d-1}$ is given by

$$\vec{j} = -D_t \vec{\nabla} c = D_t \frac{c_0}{L} \vec{e}_x, \tag{4}$$

and defines the transport diffusion coefficient D_t.

We want to understand how the anomalous $\ln t$ dependence of $D_s(t)$ in $d=2$ is reflected by D_t and if D_t decreases with the boundary roughness in the same way as D_s does. According to Malek and Coppens, D_t is not affected by the boundary roughness and thus behaves very different from self-diffusion [4,13,14]. To see if this claim is correct, we have perfomed extensive numerical calculations of D_t, where particular emphasis is given to the L dependence arising in Eq. (4).

Since the relaxation of the particle flow into a stationary state is very time consuming, it has become common to derive D_t from the probability f_t, that one single particle that starts at the left wall leaves the system at the right wall [21]. To calculate f_t, N random trajectories are considered that start at $x=0$ and end when either $x=0$ or $x=L$ is reached. By definition, f_t is the ratio between the number of particles leaving the pore at the right wall and N. Since $|\vec{j}|=c_0 f_t \langle u_x \rangle$, we obtain with Eq. (4),

$$D_t = \langle u_x \rangle f_t L, \tag{5}$$

where $\langle u_x \rangle$ is the mean velocity in the x direction of all particles when reaching the exit at the right side of the pore.

Our calculation of f_t differs from the treatment of [4], where only those particles were taken into account that penetrated into the system to some predetermined value $x_{\min} > 0$. To see, which treatment gives the correct D_t, we have calculated for small systems in $d=2$ both the stationary current density $\vec{j}$ and f_t as a function of L for several values of $x_{\min}$. This allows us to compare D_t calculated from Eq. (4) with D_t calculated from Eq. (5). The results, obtained for $\nu=0$ and one specific realization of $\nu=3$, respectively, are shown in Fig. 4. The curves calculated with Eqs. (4) and (5) only match perfectly when all particles are included in the calculation of f_t, i.e., for $x_{\min}=0$. Otherwise one obtains spurious results. Figure 4 also shows that for certain values of $x_{\min}$, the effect of the surface roughness is even canceled by the effect of $x_{\min}$, which possibly has lead to the incorrect results of [4,13,14]. Accordingly, it is essential to include all trajectories into the calculations, even if they leave the pore already after few steps. Omitting the short trajectories increases the value of f_t in an unpredictable and rather arbitrary way, such that the modified f_t cannot be used to determine the transport diffusion coefficient D_t.

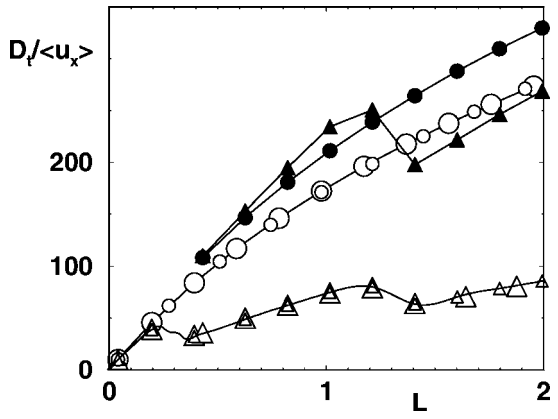

FIG. 4. $D_t/\langle u_x \rangle$ calculated from $\vec{j}$ (large open symbols) and from f_t for $x_{\min}=0$ (small open symbols) and $x_{\min}=0.4h$ (black symbols) for the $2d$ systems of $\nu=0$ (circles) and $\nu=3$ (triangles). The data from $\vec{j}$ and f_t match perfectly when $x_{\min}=0$, whereas major deviations occur for $x_{\min}>0$.

It is evident from Fig. 4 that f_t decreases with increasing roughness of the pore. To estimate the L dependence of f_t, we can use simple scaling arguments. The time t to travel a distance L scales (without logarithmic corrections) as $t \sim L^2$. Assuming that $D_t \sim f_t L$ is equivalent to D_s, we can obtain the L dependence of D_t from the t dependence of D_s and vice versa, yielding

$$D_t(L) \sim \begin{cases} \ln L^2 \sim \ln L, & d=2 \\ \text{const}, & d=3. \end{cases} \tag{6}$$

The counterintuitive increases of D_t with L in $d=2$ can be understood in the following way: With increasing, L, the number of jumps in the pore is increased and hence the probability that a very large jump will occur increases with L. In average, the particle is closer to the left wall than to the right wall and therefore the occurence of long jumps enhances f_t.

To put these scaling arguments to a direct test, we have performed extensive computer simulations of $f_t(L)$. The results are shown in Fig. 5. To reveal the logarithmic L depen-

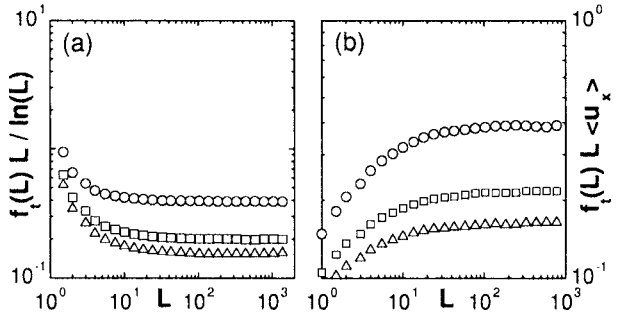

FIG. 5. (a) The scaled probability $f_t L(\ln L)^{-1}$ (averaged over 10^6 trajectories) is plotted vs the system length L for the $2d$ pores. (b) The transport diffusion coefficient $D_t = f_t L \langle u_x \rangle$ is plotted vs the system length L for the $3d$ pores. (The same symbols as in Fig. 3.)

dence of D_t in $d=2$, we plot $f_t L(\ln L)^{-1}$ vs L in Fig. 5(a). For large L, the data reach a plateau, in accordance with Eq. (6). To reveal the normal diffusion behavior in $d=3$, we have plotted the transport diffusion coefficient $D_t=f_t L\langle u_x\rangle$ versus the system size L in Fig. 5(b), where $\langle u_x\rangle \approx 0.67 u_0$ has been determined by independent numerical calculations. Again, the data reach a plateau for large values of L, in agreement with Eq. (6). From the figure, it is obvious that D_t decreases monotonically with the roughness of the pore, in remarkable disagreement with Refs. [4,13,14]. As in Fig. 3, we can see that the relative decrease of the plateaus in $d=2$ and $d=3$ with the boundary roughness is the same. Moreover, the comparison of Fig. 3(b) with Fig. 5(b) suggests that D_s and D_t in $d=3$ are indeed equivalent and the relative decrease of D_s and D_t with the boundary roughness is identical in both diffusion problems. We would like to note that in many situations, deviations from the assumption of a constant concentration gradient along the pore length [Eq. (4)] may be present, leading via Eq. (5) to the slight differences between D_s and D_t that we observe.

In summary, we have established a complete description of self- and transport diffusion (on time and on the pore length, respectively) in the Knudsen regime both in $2d$ and $3d$ pores. We have confirmed that both kinds of diffusion are identically affected by the pore morphology, exhibiting complete parallelism in slowing down with increasing surface roughness.

The authors thankfully acknowledge stimulating discussions within the DFG-NWO sponsored International Research Training Group, in particular with M.-O. Coppens, M. Kainourgiakis, F. Kapteijn, T. Steriotis, and S. Vasenkov.

[1] F. J. Keil, R. Krishna, and M.-O. Coppens, Rev. Chem. Eng. **16**, 71 (2000).

[2] J. Kärger and D. M. Ruthven, *Diffusion in Zeolites and Other Microporous Solids* (Wiley & Sons, New York, 1992).

[3] N. Y. Chen, T. F. Degnan, and C. M. Smith, *Molecular Transport and Reaction in Zeolites* (VCH, New York, 1994).

[4] K. Malek and M.-O. Coppens, Phys. Rev. Lett. **87**, 125505 (2001).

[5] G. Ertl, H. Knötzinger, and J. Weitkamp, *Handbook of Heterogeneous Catalysis* (Wiley-VCH, Chichester, 1997).

[6] F. Schüth, K. S. W. Sing, and J. Weitkamp, *Handbook of Porous Solids* (Wiley-VCH, Weinheim, 2002).

[7] R. Krishna, B. Smit, and S. Calero, Chem. Soc. Rev. **31**, 185 (2002).

[8] B. Coasne, A. Grosman, C. Ortega, and M. Simon, Phys. Rev. Lett. **88**, 256102 (2002); D. Wallacher, N. Kunzner, D. Kovalev, N. Korr, and K. Knorr, *ibid.* **92**, 195704 (2004).

[9] J. H. Sun, Z. Shan, Th. Maschmeyer, and M.-O. Coppens, Langmuir **19**, 8395 (2003); A. Corma, J. Catal. **216**, 298 (2003).

[10] H. Jobic, in *Recent Advances in Gas Separation by Microporous Membranes*, edited by N. Kanellopoulos (Elsevier, Amsterdam, 2000), p. 109.

[11] P. T. Callaghan, *Principles of NMR Microscopy* (Clarendon Press, Oxford, 1991), p. 492.

[12] U. Schemmert, J. Kärger, C. Krause, R. A. Rakoczy, and J. Weitkamp, Europhys. Lett. **46**, 204 (1999).

[13] K. Malek and M.-O. Coppens, J. Chem. Phys. **119**, 2801 (2003).

[14] K. Malek and M.-O. Coppens, Colloids Surf., A **206**, 335 (2002).

[15] M. Carrascosa, F. Cusso, and F. Agullo-Lopez, Eur. J. Phys. **6**, 183 (1985).

[16] S. B. Santra and B. Sapoval, Phys. Rev. E **57**, 6888 (1998).

[17] D. ben-Avraham and S. Havlin, *Diffusion and Reactions in Fractals and Disordered Systems* (Cambridge University Press, Cambridge, 2000).

[18] G. Zumofen and J. Klafter, Phys. Rev. E **47**, 851 (1993).

[19] J. Klafter, M. F. Shlesinger, and G. Zumofen, Phys. Today **49**(2), 33 (1996).

[20] For smooth pores, $t=\Sigma_{i=1}^{N} t_i = h u_0^{-1} \Sigma_{i=1}^{N} (\cos\varphi_i)^{-1}$. For uncorrelated x_i, $\langle x^2\rangle = \langle (\Sigma_{i=1}^{N} x_i)^2\rangle = \langle \Sigma_{i=1}^{N} x_i^2\rangle = h^2 \langle \Sigma_{i=1}^{N} \tan^2\varphi\rangle$ in $d=2$. For $N \gg 1$, we may pass to the continuum limit $\langle x^2\rangle = N h^2 \int_0^{\varphi_{\max}} P(\varphi) \tan^2\varphi d\varphi$, where $\varphi_{\max}$ is the maximum angle that occurs during N steps. One can show using some algebra that $\varphi_{\max} = \arcsin(1-2/N)$. Calculating the above integral, we find $D_s \sim \ln t$. It is interesting to note that a homogeneous distribution of φ would lead to $D_s \sim t/\ln t$.

[21] J. W. Evans, M. H. Abbasi, and A. Sarin, J. Chem. Phys. **72**, 2967 (1980).